Cell. Mol. Life Sci. 65 (2008) 4028 – 4038
1420-682X/08/244028-11
DOI 10.1007/s00018-008-8530-3

Cellular and Molecular Life Sciences

Research Article

Preferences of transmembrane helices for cooperative amplification of $G_\alpha s$ and $G_\alpha q$ signaling of the thyrotropin receptor

H. Jaeschke[a,†], G. Kleinau[b,†], J. Sontheimer[a], S. Mueller[a], G. Krause[b] and R. Paschke[a,*]

[a] III. Medical Department, University of Leipzig, Philipp-Rosenthalstr. 27, 04103 Leipzig (Germany), Fax: +49-341-9713209, e-mail: Ralf.Paschke@medizin.uni-leipzig.de
[b] Leibniz-Institut für Molekulare Pharmakologie, Robert-Rössle-Str.10, 13125 Berlin (Germany)

Received 29 August 2008; received after revision 29 September 2008; accepted 7 October 2008
Online First 8 November 2008

Abstract. The majority of constitutively activating mutations (CAMs) of the thyroid-stimulating hormone receptor display a partially activated receptor. Thus, full receptor activation requires a multiplex activation process. To define impacts of different transmembrane helices (TMHs) on cooperative signal transduction, we combined single CAMs in particular TMHs to double mutations and measured second messenger accumulation of the $G_\alpha s$ and the $G_\alpha q$ pathway. We observed a synergistic increase for basal activity of the $G_\alpha s$ pathway, for all characterized double mutants except for two combinations. Each double mutation, containing CAMs in TMH2, 6 and 7 showed the highest constitutive activities, suggesting that these helices contribute most to $G_\alpha s$-mediated signaling. No single CAM revealed constitutive activity for the $G_\alpha q$ pathway. The double mutations with CAMs from TMH1, 2, 3 and 6 also exhibited increase for basal $G_\alpha q$ signaling. Our results suggest that TMH2, 6, 7 show selective preferences towards $G_\alpha s$ signaling, and TMH1, 2, 3, 6 for $G_\alpha q$ signaling.

Keywords. G protein-coupled receptors, constitutively activating mutations, synergism, G protein selectivity, thyroid-stimulating hormone receptor.

Introduction

The thyrotropin hormone receptor (TSHR) belongs, together with the luteinizing hormone/chorionic gonadotropin receptor (LHCGR) and follitropin hormone receptor (FSHR), to the subfamily of glycoprotein hormone receptors (GPHR). The GPHRs, in turn, are part of the family class A rhodopsin-like G protein-coupled receptors (GPCRs) [1–4]. The main characteristic of this large GPCR family is the common structure of seven transmembrane helices (TMHs) connected by three extracellular loops (ECLs) and three intracellular loops (ICLs). This structure penetrates the membrane like a serpent and is, therefore, called serpentine domain. GPHRs are different from other class A receptors since they are characterized by a large extracellular domain, which is responsible for extracellular binding of their natural high molecular weight agonist the glycoprotein hormone [5].

The TSHR signals mainly *via* $G_\alpha s$, but at higher ligand concentrations the TSHR also triggers the $G_\alpha q$-mediated pathway [6]. For the human (h)TSHR a

† These authors contributed equally to this work.
* Corresponding author.

high number of constitutively activating mutations (CAMs) are known (www.fmp-berlin.de/ssfa, http://innere.uniklinikum-leipzig.de/tsh [7]). The majority of CAMs affect $G_\alpha s$ activation. Only few CAMs located at position S281 (V, M, I) in the ectodomain, I486F and M in ECL1 and I568T in ECL2 are reported to activate both the $G_\alpha s$ and the $G_\alpha q$ pathway [8, 9]. CAMs are related to human diseases, and somatic and germline *in vivo* TSHR mutations result in hyperthyroidism [6, 10].

To reflect the molecular background of constitutive activity induced by mutations, the prevailing concept is that different CAMs in different regions induce different receptor conformations distinct from the conformation mediated by the native ligand. This is also supported by the circumstance that CAMs for the TSHR do not show total activity because they can still be activated by the native ligand.

However, some of the CAMs display a much higher basal signaling than others with a very small capacity for additional TSH stimulation. This very likely depends on the biochemical and physical properties of the respective amino acid side chain substitutions, which will determine the spatial environment and mechanism of constitutive activation [11, 12]. We hypothesized in this study that single CAMs induce only a local and singular signaling event, whereas the binding and action of the native ligand TSH leads to a more complex and pronounced relocation and/or orientation of several relevant signaling structures. This multiplex event finally results in full receptor activation and is followed by a maximum of G protein activation. We recently demonstrated a synergistic and cooperative effect of CAMs at the extracellular side of the TSHR [13].

To test our hypothesis at the transmembrane region, we postulated in this study that combining single CAMs in the TMHs to double mutants should increase the level of basal activity of the mutated receptors compared with the single mutations thereby mimicking additional conformational changes of the TMHs.

Our major goal was therefore to clarify which combination of CAMs in which TMH would be characterized by the strongest influence on synergistic signaling efficacy for $G_\alpha s$ or $G_\alpha q$. We systematically combined known CAMs from the TMHs of the TSHR (TMH1: $G431^{1.49}S$ [14]; TMH2: $M453^{2.43}T$ [15]; TMH3: $L512^{3.43}Q$ [16]; TMH5: $Y601^{5.58}N$ [17, 18]; TMH6: $A623^{6.34}V$ [19]; TMH7: $N674^{7.49}D$ [20, 21]) with each other to double mutants and characterized the constructs for their signaling properties. Our results revealed that combination of single CAMs in the TSHR to double mutations leads to synergistic increase of constitutive activity for the $G_\alpha s$-mediated pathway. Interestingly, none of the single mutations displayed constitutive activity for $G_\alpha q$ signaling. However, combining particular single mutations also results in constitutive activity for the $G_\alpha q$-mediated pathway. We show that cooperative effects between the TMHs in the TSHR are not restricted to a subset of TMHs. Moreover, our results demonstrate common but also selective preferences of particular TMHs for signal transduction towards $G_\alpha s$ and $G_\alpha q$.

Material and methods

Site-directed mutagenesis. The TSHR mutants were constructed by PCR mutagenesis using the human TSHR-pcDNA3.1(–)/hygro as template as previously described [22]. Mutated TSHR sequences were verified by dideoxy sequencing with dRhodamine Terminator Cycle Sequencing chemistry (ABI Advanced Biotechnologies, Inc., Columbia, MD).

Cell culture and transient expression of mutant TSHRs. COS-7 cells were grown in Dulbecco's modified Eagle's medium (DMEM) supplemented with 10% FCS, 100 U/ml penicillin and 100 µg/ml streptomycin (Gibco Life technologies, Paisley, UK) at 37°C in a humidified 5% CO_2 incubator. Cells were transiently transfected in 24-well plates (0.5×10^5 cells per well) with 300 ng DNA per well using the GeneJammer® Transfection Reagent (Stratagene, Amsterdam, The Netherlands).

FACS analyses. The TSHR cell surface expression level was quantified on a FACS flow cytometer. Transfected cells were detached from the dishes with 1 mM EDTA and 1 mM EGTA in PBS and transferred into Falcon 2054 tubes. Cells were washed once with PBS and then incubated at 4°C for 1 h with a 1:400 dilution of a mouse anti human TSHR antibody (2C11, 10 mg/l, Serotec Ltd., Oxford, UK) in the same buffer. Cells were washed twice and incubated at 4°C for 1 h with a 1:200 dilution of fluorescein-conjugated $F(ab')_2$ rabbit anti mouse IgG (Serotec). Before FACS analysis (FACScan Becton Dickinson and Co., Franklin Lakes, NJ, USA), cells were washed twice and then fixed with 1% paraformaldehyde. Receptor expression was determined by the mean fluorescence intensity (MFI). The wild-type (wt) TSHR was set at 100% and receptor expression of the mutants was calculated according to this. The percentage of signal positive cells corresponds to transfection efficiency, which was approximately 50–60% of viable cells for each mutant.

cAMP accumulation assay. For cAMP assays cells were grown and transfected in 24-well plates. At 48 h after transfection, cells were incubated in the absence or presence of 100 mU/ml bTSH (Sigma) in serum-free medium supplemented with 1 mM IBMX (Sigma) for 1 h. Reactions were terminated by aspiration of the medium. The cells were washed once with ice-cold PBS and then lysed by addition of 0.1 N HCl. Supernatants were collected and dried. cAMP content of the cell extracts was determined using the cAMP AlphaScreen™ Assay (PerkinElmer) according to the manufacturer's instructions.

Linear regression analysis of constitutive activity as a function of TSHR expression (slopes). The magnitude of basal activity for several GPCRs is reported to depend on the receptor number expressed on the cell surface. To investigate the mutation's constitutive activity independently from their cell surface expression, we performed linear regression analyses. COS-7 cells were transiently transfected in 24-well plates (0.5×10^5 cells per well) with increasing concentrations of wt or mutant TSHR plasmid DNA (50, 100, 150, 200, 250 and 300 ng per well). The total DNA amount for the determination of constitutive activity by linear regression analyses was kept constant by cotransfection with empty vector to the amount of the highest DNA concentration of 300 ng per well. For determination of the transfected constructs see "FACS analyses". The arbitrary fluorescence units for Mock transfected cells using 50, 100, 150, 200, 250, 300 ng plasmid DNA were subtracted from the respective values for each mutant. Basal cAMP formation as a function of receptor expression was analyzed according to Ballesteros and co-workers [23] using the linear regression module of GraphPad Prism 4 for Windows. Second messenger signaling might be compartmentalized. The study of localized signaling together with temporal aspects will require single receptor tracking by new imaging techniques.

Activation of inositol phosphate (IP) formation. Transfected COS-7 cells were incubated with 2 μCi [myo-^{3}H]inositol (Amersham Biosciences, Braunschweig, Germany) for 6 h. Thereafter, cells were incubated with serum-free DMEM containing 10 mM LiCl and 100 mU TSH/ml for the stimulation of the transfected cells. Evaluation of basal and TSH-induced increases in intracellular IP levels was performed by anion exchange chromatography as previously described [24]. IP values were expressed as the percentage of radioactivity incorporated from [^{3}H]IP-1 to -3 over the sum of radioactivity incorporated in IPs and phosphatidylinositol.

Molecular modeling. The structural model of the serpentine domain of hTSHR was generated based on the X-ray structures of the bovine rhodopsin (PDB entry codes: 1GZM [25]; 2I35 [26]; 2J4Y [27]) and refined using the recently solved crystal structures of the partially active β2-adrenergic receptor (PDB entry code: 2RH1 [28]; 2R4R [29]). Several TSHR-specific corrections were made, such as regular helix extensions in TMH2 and TMH5 of the TSHR instead of structural bulges in the TMH2 and 5 of rhodopsin caused by the specific side chains that are not present in TSHR (two consecutive threonines in TMH2 and a proline in TMH5). Loops were added by best fit and homology to fragments of other proteins (from PDB). Gaps of missing residues in the loops of the template structure were closed by the 'Loop Search' tool implemented in Sybyl 7.2.5 (Tripos Inc., St. Louis, Missouri, 63144, USA). The sheet-like fold of the ECL2 and its localization was kept as in rhodopsin based on the high sequence homology and the rhodopsin structure-consistent results of diverse studies at other GPCRs [30–32] and the TSHR [33]. The different length and the lower sequence similarity with the TSHR as well as the additional disulfide bridge make the b2AR a less likely template for the ECL2 conformation. The wt receptors as well as the double mutated receptor models were minimized and validated. Conjugate gradient minimizations for all models were performed until converging at a termination gradient of 0.05 kcal/(mol*Å), the AMBER 7.0 force field [34] was used. Quality and stability of the model were validated by checking the geometry by PROCHECK [35] and during a molecular dynamics simulation of 2 ns (overall backbone RMSD 1.8 Å).

Statistics. Statistical analysis was carried out using the Mann-Whitney nonparametric *t* test using GraphPad Prism 4 for Windows.

Results

Utilizing a GPHR mutation phenotype resource ([7], www.fmp-berlin.de/ssfa), we selected CAMs of the TSHR that are characterized by following properties: (1) constitutive activity >200% compared with the basal wt TSHR (set at 100%); (2) cell surface expression of single mutants greater than 50% compared with the wt TSHR (set at 100%); and (3) localization in the transmembrane region. Five of considered mutants G431$^{1.49}$S in TMH1 [14], M453$^{2.43}$T in TMH2 [15], L512$^{3.43}$Q in TMH3 [16], Y601$^{5.58}$N in TMH5 [17, 18] and A623$^{6.34}$V in TMH6 [19] have been reported in relation to non-autoimmune hyperthyroidism, whereas mutation

N674$^{7.49}$D in TMH7 is an *in vitro* mutation [20, 21]. TMH4 was excluded from the study as there is no known CAM in this particular structure. The selected mutants and their relative location within the TMHs are schematically shown in Figure 1. We generated these single mutations and further created double mutants with every possible combination to each other. All mutations were characterized regarding cell surface expression, basal and TSH-mediated cAMP production, linear regression analyses of constitutive activity and formation of IPs.

Desensitization and internalization are processes that have an important impact on the down-regulation of CAMs. Although our experiments were performed in a heterologous cell system where TSHRs were highly overexpressed and where the endogenous pool of regulatory molecules was limited, we cannot completely exclude influences of internalized or desensitized receptors in our study on cell surface expression and signaling.

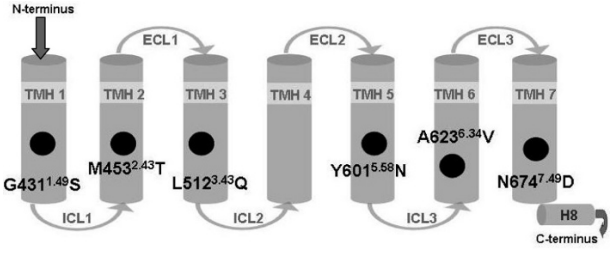

Figure 1. Schematic representation of the transmembrane portion and intracellular loops (ICLs) of the thyrotropin hormone receptor (TSHR) with relative locations of investigated constitutively activating mutations (CAMs).

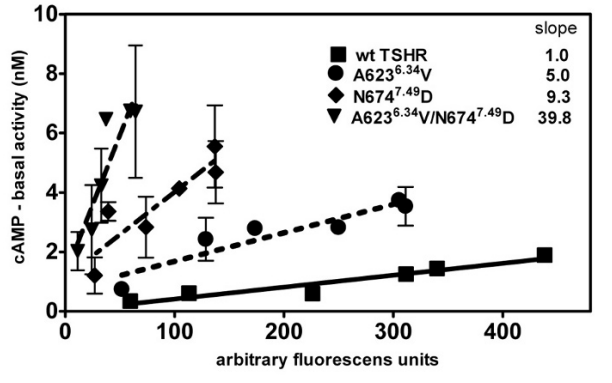

Figure 2. Determination of the constitutive activity independently from the cell surface expression. As a representative example, the combination between TMH6/7 is shown. Slopes were calculated using the GraphPad Prism 4 software for windows. The slope for the wild-type (wt) TSHR was set at 1 and the slopes for the mutants were calculated according to this. Slopes are presented as means ± standard deviation (SD) of at least three independent experiments (n=3), each performed in duplicate.

Cell surface expression. The single mutants exhibited expression levels in a range of 46–106 % compared with the wt TSHR (set at 100 %) (Table 1). Thereby, L512$^{3.43}$Q and A623$^{6.34}$V revealed, with 106 % and 101 %, respectively, the highest cell surface expression of all characterized mutants followed by G431$^{1.49}$S with 91 % (Table 1). M452$^{2.43}$T showed a reduced expression of 67 % and Y601$^{5.58}$N and N674$^{7.49}$D exhibited, with 46 % and 48 %, the lowest levels of receptor expression (Table 1). The best expressed double mutant with 75 % was the combination between L512$^{3.43}$Q and A623$^{6.34}$V of TMH3 and 6. The other constructs were expressed between 12 % and 58 % compared with the wt TSHR (Table 1). The combination TMH5/7 could not be further characterized as this double mutant showed no expression leading to limitations regarding cAMP and IP measurements.

Maximum of cAMP accumulation stimulated by TSH. Measurement of cAMP accumulation after TSH treatment revealed for the single mutants comparable data as determined for the wt TSHR. Only mutant Y601$^{5.58}$N showed a significantly decreased cAMP formation to 50 % (Table 1). Half of the double mutants responded well after ligand-induced activation, whereas the others showed a reduced increase in cAMP accumulation compared with the wt TSHR (Table 1).

Basal cAMP accumulation. All mutants were constitutively active showing significantly increased basal values when compared with the wt TSHR (Table 1). To characterize the mutants' constitutive activity independently from their cell surface expression, we performed linear regression analyses of basal activity. As shown in Table 1, most of the single mutants exhibited slopes of circa 5-fold, whereas N674$^{7.49}$D in TMH7 displayed a higher slope of 9.3-fold (wt TSHR set at 1) (Fig. 2). Combining the single CAMs led to a remarkable increase of constitutive activity when compared to the values obtained for the single mutations (Fig. 3A). The strongest effects were determined for the four combinations with N674$^{7.49}$D in TMH7 and the combination TMH5/6 with slopes between 27.4- and 39.8-fold including mutant A623$^{6.34}$V/N674$^{7.49}$D (TMH6/7), which displayed the highest slope of 39.8-fold of all characterized constructs. Also the mutants of TMH1/2, TMH2/5 and TMH2/6 with 23.4–25.5-fold as well as TMH1/3, TMH1/6 and TMH2/3 with slopes in a range of 16.3–20.2-fold showed an increase in constitutive activity (Table 1 and Fig. 2).

However, two constructs gave different results. Double mutants L512$^{3.43}$Q/Y601$^{5.58}$N (TMH3/5) and

Table 1. Functional characterization of thyrotropin hormone receptor (TSHR) single and double mutants.

Construct	Localization	Cell surface expression	cAMP accumulation			IP accumulation [IPs (%IP/IPs + PI)]	
		FACS % of wt TSHR	basal	100 mU/ml TSH	Constitutive activity (slope)	basal	100 mU/ml TSH
wt TSHR	–	100	1	13.3 ± 0.9	1	3.7 ± 0.5	41.1 ± 1.7
pcDNA	–		0.3 ± 0.1	0.4 ± 0.1	–	3.0 ± 0.3	3.3 ± 0.3
G431$^{1.49}$S	TMH1	90 ± 3^{c}	4.3 ± 0.6^{b}	13.1 ± 2.9	4.9 ± 0.5^{a}	2.7 ± 0.2	45.3 ± 2.0
M453$^{2.43}$T	TMH2	66 ± 2^{a}	5.7 ± 0.5^{a}	11.2 ± 1.4	5.2 ± 0.8^{b}	3.8 ± 0.5	35.6 ± 1.7
S505$^{3.36}$N	TMH3	81 ± 3^{b}	5.0 ± 0.8^{a}	14.5 ± 2.2	4.5 ± 0.3^{b}	2.8 ± 0.3	49.6 ± 7.1
L512$^{3.43}$Q	TMH3	106 ± 5	3.7 ± 0.7^{b}	11.5 ± 1.0	4.5 ± 0.7^{b}	3.4 ± 0.7	21.5 ± 0.4^{b}
Y601$^{5.58}$N	TMH5	48 ± 2^{a}	4.8 ± 0.9^{b}	7.1 ± 0.9^{b}	5.9 ± 0.1^{b}	3.4 ± 0.2	8.5 ± 0.2^{b}
A623$^{6.34}$V	TMH6	101 ± 2	4.5 ± 0.3^{a}	16.2 ± 2.7	5.0 ± 0.7^{a}	3.3 ± 0.5	39.0 ± 1.7
N674$^{7.49}$D	TMH7	46 ± 2^{a}	3.8 ± 0.3^{a}	13.5 ± 2.2	9.3 ± 1.7^{b}	2.6 ± 0.2	19.0 ± 0.4^{b}
G431$^{1.49}$S/ M453$^{2.43}$T	TMH1/TMH2	28 ± 2^{a}	6.4 ± 1.3^{b}	10.0 ± 2.2	23.4 ± 5.9^{a}	12.0 ± 1.0^{b}	39.5 ± 1.0
G431$^{1.49}$S/L512$^{3.43}$Q	TMH1/TMH3	50 ± 1^{a}	5.4 ± 0.8^{b}	7.3 ± 1.0^{b}	17.1 ± 2.3^{a}	5.7 ± 0.7^{c}	23.4 ± 1.7^{b}
G431$^{1.49}$S/Y601$^{5.58}$N	TMH1/TMH5	21 ± 1^{b}	3.9 ± 0.6^{c}	4.9 ± 0.7^{b}	14.7 ± 3.5^{a}	2.5 ± 0.3	3.6 ± 0.1^{a}
G431$^{1.49}$S/A623$^{6.34}$V	TMH1/TMH6	55 ± 2^{a}	5.0 ± 1.0^{b}	10.3 ± 1.7	16.3 ± 2.0^{a}	3.7 ± 0.6	34.3 ± 2.1
G431$^{1.49}$S/N674$^{7.49}$D	TMH1/TMH7	23 ± 2^{a}	5.8 ± 0.3^{b}	14.1 ± 1.6	30.1 ± 6.5^{a}	2.8 ± 0.0	12.1 ± 0.4
M453$^{2.43}$T/L512$^{3.43}$Q	TMH2/TMH3	49 ± 2^{a}	6.0 ± 1.1^{a}	7.7 ± 0.4^{b}	20.2 ± 2.6^{a}	6.6 ± 0.5^{b}	27.5 ± 2.0^{b}
M453$^{2.43}$T/ Y601$^{5.58}$N	TMH2/TMH5	19 ± 1^{a}	5.6 ± 0.1^{c}	6.7 ± 0.3^{b}	25.5 ± 6.0^{a}	3.3 ± 0.1	3.5 ± 0.1^{a}
M453$^{2.43}$T/A623$^{6.34}$V	TMH2/TMH6	31 ± 2^{a}	7.1 ± 1.3^{a}	7.7 ± 1.3^{b}	24.0 ± 5.6^{a}	9.6 ± 0.5^{b}	34.5 ± 1.5
M453$^{2.43}$T/N674$^{7.49}$D	TMH2/TMH7	12 ± 1^{a}	7.0 ± 1.2^{b}	8.1 ± 1.6^{c}	33.3 ± 3.6^{a}	3.1 ± 0.1	7.5 ± 0.1^{b}
S505$^{3.36}$N/Y601$^{5.58}$N	TMH3/TMH5	26 ± 1^{a}	5.6 ± 0.3^{b}	6.3 ± 0.5^{b}	14.7 ± 3.9^{a}	5.8 ± 0.2^{c}	7.4 ± 0.2^{b}
S505$^{3.36}$N/A623$^{6.34}$V	TMH3/TMH6	58 ± 2^{b}	6.7 ± 1.0^{c}	10.1 ± 1.1	14.2 ± 2.8^{a}	10.7 ± 0.3^{b}	43.1 ± 1.2
L512$^{3.43}$Q/Y601$^{5.58}$N	TMH3/TMH5	51 ± 4^{b}	2.7 ± 0.2^{c}	5.0 ± 0.7^{b}	4.4 ± 0.3^{b}	2.3 ± 0.1	5.0 ± 0.3^{a}
L512$^{3.43}$Q/A623$^{6.34}$V	TMH3/TMH6	75 ± 5^{a}	7.3 ± 1.6^{a}	10.0 ± 2.7	7.8 ± 1.4^{a}	3.3 ± 0.3	17.1 ± 1.7^{b}
L512$^{3.43}$Q/N674$^{7.49}$D	TMH3/TMH7	20 ± 2^{a}	5.9 ± 0.4^{b}	12.6 ± 2.4	27.4 ± 7.7^{a}	2.3 ± 0.2	3.1 ± 0.5^{a}
Y601$^{5.58}$N/A623$^{6.34}$V	TMH5/TMH6	23 ± 2^{b}	3.3 ± 0.2^{c}	6.2 ± 1.3^{b}	30.0 ± 1.1^{a}	2.7 ± 0.7	4.0 ± 0.3^{a}
A623$^{6.34}$V/N674$^{7.49}$D	TMH6/TMH7	23 ± 2^{a}	7.1 ± 2.5^{a}	11.1 ± 1.2	39.8 ± 10.9^{a}	3.3 ± 0.0	9.7 ± 0.5^{b}

COS-7 cells were transfected with wild-type (wt) TSHR or various mutant TSHRs. The vector pcDNA3.1(–)/hygromycin was used as a control. The TSHR is characterized by an elevated cAMP level compared to the control vector alone [59]. Therefore, cAMP accumulation is expressed relative to wt TSHR basal level. TSH-mediated levels of cAMP and inositol phosphate (IP) accumulation were determined after treatment of cells with 100 mU/ml bTSH. Expression of wt and mutant TSHRs were quantified on a FACS flow cytometer. Data are given as mean ± SD of at least three independent experiments (n=3), each carried out in duplicate. Constitutive activity by linear regression analyses was determined for G_{α}s and not for G_{α}q signaling due to the fact that the wt TSHR do not show elevated G_{α}q levels.
[a] $p<0.001$, [b] p=0.001–0.01, [c] p=0.01–0.05.

L512$^{3.43}$Q/A623$^{6.34}$V (TMH3/6) revealed no significant increase in constitutive activity compared to the respective single mutants (Table 1 and Fig. 3A). To test whether this finding depends on the position mutated in TMH3, we searched for a new mutant in this helix. We identified mutant S505$^{3.36}$N, which is located two turns above residue L512$^{3.43}$Q and fulfilled the criteria regarding cell surface expression and basal cAMP signaling mentioned above. Therefore, we generated three new constructs (S505$^{3.36}$N, S505$^{3.36}$N/Y601$^{5.58}$N and S505$^{3.36}$N/A623$^{6.34}$V). The single mutant S505$^{3.36}$N displayed a cell surface expression of 81 %, a basal and TSH-mediated cAMP production comparable with the other single mutants and a slope of 4.5-fold (Table 1). The double mutations S505$^{3.36}$N/Y601$^{5.58}$N and S505$^{3.36}$N/A623$^{6.34}$V revealed expression levels of 26 % and 58 %, respectively. In contrast to mutations L512$^{3.43}$Q/Y601$^{5.58}$N and L512$^{3.43}$Q/A623$^{6.34}$V, the newly generated double mutants with S505$^{3.36}$N instead of L512$^{3.43}$Q displayed with 14.7- and 14.2-fold, respectively, a much higher slope (Table 1 and Fig. 3A). This suggests that CAM L512$^{3.43}$Q prevents the receptor becoming more active by the introduction of a second mutation in TMH6.

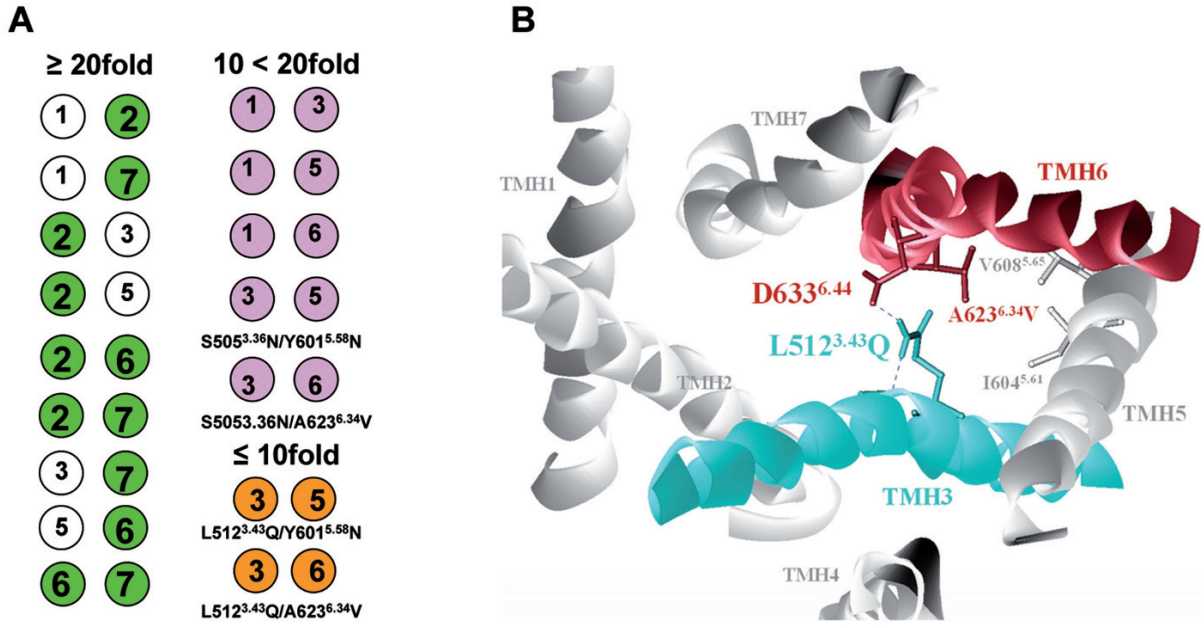

Figure 3. (*A*) Pairs of transmembrane helices (TMHs) of combined CAMs. Green circles: Combinations with a constitutive activity (slope) higher than 20-fold. TMHs with the highest impact on constitutive activity are highlighted. Magenta circles: Combinations with a slope between 10- and 20-fold. Orange circles: Combinations with a slope lower than 10-fold. (*B*) Repression of synergistic signaling by double mutation L512$^{3.43}$Q/A623$^{6.34}$V and L512$^{3.43}$Q/Y601$^{5.58}$N is caused by new H-bond side chain interactions between L512$^{3.43}$Q with D633$^{6.44}$ in TMH6 constraining interactions of TMH3 and TMH6.

IP formation. Determination of the IP formation revealed no detectable constitutive activity for the single mutants when compared with the wt TSHR. Surprisingly, combinations including mutation M452$^{2.43}$T of TMH2 (TMH1/2, TMH2/3 and TMH2/6) led to an increase of ligand-independent IP formation (Table 1), and combinations of TMH1/3 (G431$^{1.49}$S/L512$^{3.43}$Q), TMH3/5 (S505$^{3.36}$N/Y601$^{5.58}$N) and TMH3/6 (S505$^{3.36}$N/A623$^{6.34}$V) exhibited elevated basal values (Table 1 and Fig. 4B). The majority of mutants responded well to stimulation with TSH (Table 1 and Fig. 4A). Some mutants, L512$^{3.43}$Q and N674$^{7.49}$D, showed reduced IP accumulation to 50%, and Y601$^{5.58}$N exhibited only 20% IP release compared to the wt TSHR when activated by TSH.

Molecular modeling of double mutant L512$^{3.43}$Q/A623$^{6.34}$V (TMH3/6). The double mutants including CAM L512$^{3.43}$Q (TMH3) were characterized as the mutations do not reveal any synergistic influence on signaling capability compared to other double mutants. The molecular model of the TSHR including the double mutant L512$^{3.43}$Q/A623$^{6.34}$V (TMH3/6) was designed to reveal insights in this experimental result. As shown in Figure 3B, the side chain of the glutamine at position 512$^{3.43}$ is oriented towards aspartate at 633$^{6.44}$ in TMH6 and forms a hydrogen bond. This aspartate in TMH6 (D633$^{6.44}$) is known to be important for receptor activation by interactions with amino acids at TMH7 [21, 36]. Therefore, we suggest, based on our molecular model, that this new H-bond between the glutamine at position 512$^{3.43}$ in TMH3 and the aspartate at TMH6 (D633$^{6.44}$) is effective as a constraint that ties up TMH6 and thus avoids TSHR activation *via* movement of TMH6 relatively to TMH3.

Discussion

For GPCRs, several studies with rhodopsin and the β_2-adrenergic receptor suggest a change in the orientation and localization of the TMHs relative to each other during receptor activation or rather signal transduction [37–42]. However, these studies examined the impact of one or, in few cases, two helices by biophysical approaches. In this work we systematically investigated the impact on signal transduction of nearly all helices of the TSHR regarding the primary signaling pathway $G_\alpha s$ and also *via* the second pathway $G_\alpha q$ by mutagenesis using CAMs.

Synergistic signaling by CAM combinations in the TMHs of the TSHR is not limited to a subset of TMHs. By systematic combination of single CAMs in different TMHs to double mutations, our results suggest

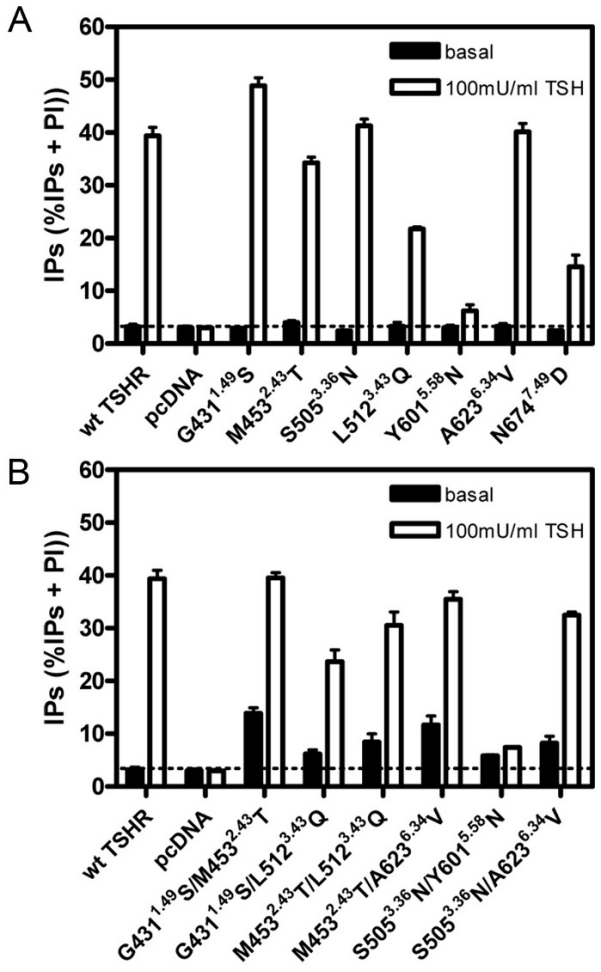

Figure 4. Functional characterization of the $G_{\alpha}q$ pathway. Data are presented as means ± SD of at least three independent experiments (n=3), each performed in duplicate. (*A*) Shown are the basal and thyroid-stimulating hormone (TSH)-mediated phenotypes for all generated double mutants and (*B*) for the double mutants displaying constitutive activity.

that simultaneous and cooperative signaling events at the TSHR are not restricted to a special subset of TMHs. Furthermore, our study shows that nearly all TMHs seem to be involved in the signal transduction process but vary in their efficacies (Table 1, Fig. 3A). The results reveal also that a multiplex TSHR activation and signal transduction complex seems to be necessary for complete receptor-mediated signaling. In a reverse interpretation this might explain why single CAMs are mostly characterized by partial receptor-mediated signaling.

Previous studies revealed synergistic increase of basal activity by sporadically combining two or three CAMs in one receptor. This was shown for CAMs in TMH3 and 6 of rhodopsin [43], for TMH2 and 3 of the Kaposi's sarcoma-associated herpes virus-GPCR [44], and for CAMs located in TMH3 and 5 and in the transition of TMH6/ECL3 in the α_1-adrenergic receptor [45]. In addition to these previous reports of synergism for limited combinations, our systematic investigation revealed both a general amplifying effect for nearly all TMH combinations and different impacts of particular TMHs on ligand-independent signaling intensities.

Different efficacies of the TMHs for signal mediation at the TSHR. The strongest increases of ligand-independent activity were measured for combinations harboring mutations in TMH2, 6 and 7, respectively. For these double mutants slopes greater than 20-fold were determined, compared to the single CAMs, suggesting that a rearrangement of these helices mediate a higher contribution for the activation of the $G_{\alpha}s$ pathway than other helices. Besides our studies on the TSHR, a fundamental role of helices 2, 6, and 7 in other GPCRs was previously suggested by experimental studies. First, biophysical investigation of structural changes during the activation of the rhodopsin or the β_2-adrenergic receptor revealed that TMH6 through the N-terminal region undergoes major displacement relative to TMH3 and that this rearrangement of TMH6 is similar, if not identical, in both characterized receptors [37, 39–42, 46].

Secondly, further evidence for the importance of TMH6 for receptor activation was provided by studies with glycoprotein hormone receptors. Mutagenesis and computational approaches for the characterization of potential helical interactions between TMH3/6 and TMH6/7 in TSHR and LHCGR revealed a complex network of H-bonds to maintain the inactive conformation. Disruption of these interactions by *in vitro* mutations led to constitutive activation in many cases, which is also reflected by a high number of pathogenic CAMs in the TMHs 3, 6 and 7 compared to other helices in these receptors [20, 21, 47–49]. Also, for the β_2-adrenergic receptor, a change in the structural orientation of TMH6 and 7 during receptor activation was observed, which most likely represents a universal feature of GPCR function [38].

Thirdly, Urizar and co-workers [49] recently provided mutational data that the release of the interaction between $D633^{6.44}$ (TMH6) and $N674^{7.49}$ (TMH7) in the TSHR is a necessary step for receptor activation and that $N674^{7.49}$ forms a new H-bond interaction with $D460^{2.50}$ of TMH2 in the activated conformation. Structural displacement of TMH2 and 7 during light-induced activation of rhodopsin was also demonstrated by electron paramagnetic resonance spectroscopy [50–52]. The finding of a participation of TMH2 in the activation process is further supported by earlier studies with the gonadotropin-releasing hormone receptor, the 5-HT_{2a} receptor and the angiotensin II

type 1 receptor [53–55]. Altogether, despite the diversity of the natural ligands and their different relative binding sites on the membrane-associated GPCRs, it seems that similar intramolecular mechanisms for activation and/or signal transduction are conserved. Interestingly, concerning the functional-structural importance of helices 3, 6 and 7, an evolutionary study using orthologs of a P2Y-like receptor (GPR34) showed that these three helices are more conserved over 450 million years of evolution compared to other TMHs [56].

Constitutive activation of the $G_\alpha q$ pathway by double mutations in the TMHs of the TSHR. The TSHR also signals *via* the $G_\alpha q$ pathway with physiological relevance, as well as *via* the $G_\alpha s$ pathway [6, 57]. To date only 6 out of 44 *in vivo* mutants are known to constitutively activate the TSHR for the $G_\alpha q$ signaling cascade (www.fmp-berlin.de/ssfa, http://innere.uni klinikum-leipzig.de/tsh, [7]). Our functional characterization of the generated constructs revealed no constitutive $G_\alpha q$ activity for the single mutations (Table 1 and Fig. 4A). However, most surprisingly, 6 of 16 double mutations showed increased basal $G_\alpha q$ activity (Table 1 and Fig. 4B). These 6 constructs represent further striking examples for synergism in signal amplification and, therefore, also for the cooperation of TMHs. Moreover, only combinations including mutations in TMH1, 2, 3 and 6 were able to induce basal $G_\alpha q$ signaling. In particular, the impact of TMH3 was much more pronounced for basal IP formation than for basal cAMP accumulation. Strikingly, compared with the $G_\alpha s$ pathway, TMH7 showed no direct influence on basal $G_\alpha q$ signaling. The different preferences of TMHs to influence $G_\alpha s$ or $G_\alpha q$ signaling suggest that, after ligand binding and activation of the receptor, different conformational states exist that contribute to G protein selectivity and activation. In the rare cases of constitutive activity for the $G_\alpha q$ pathway induced by single mutations, the change in conformation seems to be more pronounced in the case for $G_\alpha q$ activation as compared to other substitutions leading only to $G_\alpha s$ activation. These differences most likely depend on the nature of the substituted amino acid. Interestingly, these constitutively IP active mutations also exhibit exceptionally high basal cAMP activities (www.fmp-berlin.de/ssfa, http://innere.uniklinik um-leipzig.de/tsh).

However, the single mutants selected for our study showed moderately increased basal signaling and no constitutive activity for $G_\alpha q$, suggesting that the structural changes induced by these side chain alterations were not effective enough to induce constitutive activity for both pathways. It is difficult to extract molecular explanations for the constitutive activation of the $G_\alpha q$ pathway for the double mutations due to the complexity of the intramolecular network between the TMHs. Based on our receptor model, the side chain of $G431^{1.49}$ in TMH1 points towards residue $P675^{7.50}$ of the conserved NPXXY motif in TMH7. Substitution of the native $G431^{1.49}$ with serine leads to a repulsion event by van der Waals forces and consequently to a displacement of THM1 and 7 relative to each other. A similar result can be observed for mutant $M452^{2.43}T$ in TMH2. The methionine is also orientated to the NPXXY motif but opposite to $Y678^{7.53}$. Substitution of the methionine at residue $452^{2.43}$ to the branched amino acid threonine very likely leads to van der Waals contacts with $Y678^{7.53}$ and therefore to a repulsion of the two helices.

Both described actions of the single mutants were not able to induce a constitutive activation of the $G_\alpha q$ pathway. However, combination of these single substitutions could overcome the threshold for ligand-independent $G_\alpha q$ activation, most likely by the addition of the repulsion effects leading to a higher basal $G_\alpha s$ and also to constitutive $G_\alpha q$ signaling. The phenotype of a mutation in a particular transmembrane helix may be due to a direct effect on the function of the helix carrying the mutation. However, we cannot exclude that the observed synergistic effects are also mediated by indirect influences on neighboring helices, *e.g.* displacement of TMH2 and 7 relative to each other could also result in a conformational change in the two helices connecting ICL1.

We suggest that the TSHR mediates its G protein selectivity by different conformations, which can be partially overlapping for $G_\alpha s$ and $G_\alpha q$. Further experiments must clarify which particular intracellular receptor structures are necessary for the recognition of the different G protein α subunits.

Suppression of synergism by new H-bond interactions between TMH3 and TMH6. Remarkably, only two particular double mutants $L512^{3.43}Q/Y601^{5.58}N$ (TMH3/5) and $L512^{3.43}Q/A623^{6.34}V$ (TMH3/6) did not show synergistic signaling effects regarding cAMP accumulation. Their constitutive activity remained at the level of the respective single mutants (Table 1 and Fig. 3A). We concluded that the phenotypes of these constructs might be related to a position-dependent event mediated by the $L512^{3.43}Q$ substitution. To understand the molecular mechanism of this particular absence of cooperativity caused by $L512^{3.43}Q$, we performed molecular modeling studies. We showed that instead of leucine, the substituted hydrophilic side chain glutamine formed a new H-bond interaction directly with $D633^{6.44}$ in an opposite

location at TMH6 and led to a fixation of TMH3 and 6 in a partially active conformation (Fig. 3B). This suggests that the new H-bond formation of D633$^{6.44}$ very likely leads to an immediate abrogation of the native H-bond interaction between D633$^{6.44}$ (TMH6) and N674$^{7.49}$ (TMH7) known to be sensitive for constitutive receptor activation [20, 21, 49]. Relating to the double mutation L512$^{3.43}$Q/A623$^{6.34}$V, the introduction of the second mutation A623$^{6.34}$V near the cytoplasmic site of TMH6 cannot overcome the constraint caused by L512$^{3.43}$Q since the interaction of L512$^{3.43}$Q with D633$^{6.44}$ prevents further displacement of TMH6 during the activation process. Therefore, we generated further double mutants, which contained S505$^{3.36}$N instead of L512$^{3.43}$Q. S505$^{3.36}$N cannot interfere with D633$^{6.44}$ since it is located two turns above L512$^{3.43}$ in TMH3. Indeed, combinations S505$^{3.36}$N/Y601$^{5.58}$N and S505$^{3.36}$N/A623$^{6.34}$V displayed synergism for signal amplification of basal ligand-independent G_{α}s signaling (Table 1 and Fig. 3A). These data indicate the intramolecular mechanisms by which the constitutively activating *in vivo* mutation L512$^{3.43}$Q leads to hyperthyroidism. Furthermore, they emphasize the role for the intramolecular H-bond network between the TMHs for maintaining the receptor in the inactive state.

Taken together, our results show that several double mutants in the transmembrane region cause synergistic effects regarding ligand-independent G_{α}s-mediated signaling at the TSHR. More important, for the first time also for the G_{α}q pathway, synergistic signaling effects were determined for double mutations in the TSHR. Surprisingly, in contrast to previous observations for other GPCRs, our approach of double mutant design by combining single CAMs in the helices with each other, reveals that synergistic signaling effects at the TSHR are not restricted to a focused and limited subset of TMHs. In agreement with observations for other GPCRs, like the very recent data about the opioid receptor [58], we conclude that multiple conformational changes in the structural arrangement of the TMHs are necessary for receptor activation and signal transduction. In addition, our results suggest that conformational changes caused at TMH2, 6 and 7 have a higher impact on G_{α}s-mediated signaling, whereas TMH1, 2, 3 and 6 are essential for G_{α}q activation.

Acknowledgements. We would like to thank Saskia Fiedler and Eileen Bösenberg for their excellent technical assistance. This study was supported by DFG Projects (Pa423/14–1; Kr1273/2–1) and a Formel-1 grant of the Medical Faculty, University of Leipzig (NML Formel.1–98).

1 Simoni, M., Gromoll, J. and Nieschlag, E. (1997) The follicle-stimulating hormone receptor: Biochemistry, molecular biology, physiology, and pathophysiology. Endocr. Rev. 18, 739–773.
2 Szkudlinski, M. W., Fremont, V., Ronin, C. and Weintraub, B. D. (2002) Thyroid-stimulating hormone and thyroid-stimulating hormone receptor structure-function relationships. Physiol. Rev. 82, 473–502.
3 Ascoli, M., Fanelli, F. and Segaloff, D. L. (2002) The lutropin/choriocrctnadotropin receptor, a 2002 perspective. Endocr. Rev. 23, 141–174.
4 Vassart, G., Pardo, L. and Costagliola, S. (2004) A molecular dissection of the glycoprotein hormone receptors. Trends Biochem. Sci. 29, 119–126.
5 Fan, Q. R. and Hendrickson, W. A. (2005) Structure of human follicle-stimulating hormone in complex with its receptor. Nature 433, 269–277.
6 Paschke, R. and Ludgate, M. (1997) The thyrotropin receptor in thyroid diseases. N. Engl. J. Med. 337, 1675–1681.
7 Kleinau, G., Brehm, M., Wiedemann, U., Labudde, D., Leser, U. and Krause, G. (2007) Implications for molecular mechanisms of glycoprotein hormone receptors using a new sequence-structure-function analysis resource. Mol. Endocrinol. 21, 574–580.
8 Jaeschke, H., Neumann, S., Kleinau, G., Mueller, S., Claus, M., Krause, G. and Paschke, R. (2006) An aromatic environment in the vicinity of serine 281 is a structural requirement for thyrotropin receptor function. Endocrinology 147, 1753–1760.
9 Parma, J., VanSande, J., Swillens, S., Tonacchera, M., Dumont, J. and Vassart, G. (1995) Somatic mutations causing constitutive activity of the thyrotropin receptor are the major cause of hyperfunctioning thyroid adenomas – Identification of additional mutations activating both the cyclic adenosine-3', 5'-monophosphate and inositol phosphate-Ca^{2+} cascades. Mol. Endocrinol. 9, 725–733.
10 Schoneberg, T., Schulz, A., Biebermann, H., Hermsdorf, T., Rompler, H. and Sangkuhl, K. (2004) Mutant G-protein-coupled receptors as a cause of human diseases. Pharmacol. Ther. 104, 173–206.
11 Kenakin, T. (2005) The physiological significance of constitutive receptor activity. Trends Pharmacol. Sci. 26, 603–605.
12 Parnot, C., Miserey-Lenkei, S., Bardin, S., Corvol, P. and Clauser, E. (2002) Lessons from constitutively active mutants of G protein-coupled receptors. Trends Endocrinol. Metab. 13, 336–343.
13 Kleinau, G., Jaeschke, H., Mueller, S., Raaka, B. M., Neumann, S., Paschke, R. and Krause, G. (2008) Evidence for cooperative signal triggering at the extracellular loops of the TSH receptor. FASEB J. 22, 2798–2808.
14 Biebermann, H., Schoneberg, T., Hess, C., Germak, J., Gudermann, T. and Gruters, A. (2001) The first activating TSH receptor mutation in transmembrane domain 1 identified in a family with nonautoimmune hyperthyroidism. J. Clin. Endocrinol. Metab. 86, 4429–4433.
15 deRoux, N., Polak, M., Couet, J., Leger, J., Czernichow, P., Milgrom, E. and Misrahi, M. (1996) A neomutation of the thyroid-stimulating hormone receptor in a severe neonatal hyperthyroidism. J. Clin. Endocrinol. Metab. 81, 2023–2026.
16 Trulzsch, B., Krohn, K., Wonerow, P., Chey, S., Holzapfel, H. P., Ackermann, F., Fuhrer, D. and Paschke, R. (2001) Detection of thyroid-stimulating hormone receptor and G(s)alpha mutations: In 75 toxic thyroid nodules by denaturing gradient gel electrophoresis. J. Mol. Med. 78, 684–691.
17 Arseven, O. K., Wilkes, W. P., Jameson, J. L. and Kopp, P. (2000) Substitutions of tyrosine 601 in the human thyrotropin receptor result in increase or loss of basal activation of the cyclic adenosine monophosphate pathway and disrupt coupling to G(q/11). Thyroid 10, 3–10.
18 Claeysen, S., Govaerts, C., Lefort, A., Van Sande, J., Costagliola, S., Pardo, L. and Vassart, G. (2002) A conserved Asn in TM7 of the thyrotropin receptor is a common requirement for activation by both mutations and its natural agonist. FEBS Lett. 517, 195–200.

19 Paschke, R., Tonacchera, M., VanSande, J., Parma, J. and Vassart, G. (1994) Identification and functional-characterization of two new somatic mutations causing constitutive activation of the thyrotropin receptor in hyperfunctioning autonomous adenomas of the thyroid. J. Clin. Endocrinol. Metab. 79, 1785–1789.

20 Govaerts, C., Lefort, A., Costagliola, S., Wodak, S. J., Ballesteros, J. A., Van Sande, J., Pardo, L. and Vassart, G. (2001) A conserved Asn in transmembrane helix 7 is an on/off switch in the activation of the thyrotropin receptor. J. Biol. Chem. 276, 22991–22999.

21 Neumann, S., Krause, G., Chey, S. and Paschke, R. (2001) A free carboxylate oxygen in the side chain of position 674 in transmembrane domain 7 is necessary for TSH receptor activation. Mol. Endocrinol. 15, 1294–1305.

22 Jaschke, H., Neumann, S., Moore, S., Thomas, C. J., Colson, A. O., Costanzi, S., Kleinau, G., Jiang, J. K., Paschke, R., Raaka, B. M., Krause, G. and Gershengorn, M. C. (2006) A low molecular weight agonist signals by binding to the transmembrane domain of thyroid-stimulating hormone receptor (TSHR) and luteinizing hormone/chorionic gonadotropin receptor (LHCGR). J. Biol. Chem. 281, 9841–9844.

23 Ballesteros, J. A., Jensen, A. D., Liapakis, G., Rasmussen, S. G. F., Shi, L., Gether, U. and Javitch, J. A. (2001) Activation of the beta(2)-adrenergic receptor involves disruption of an ionic lock between the cytoplasmic ends of transmembrane segments 3 and 6. J. Biol. Chem. 276, 29171–29177.

24 Berridge, M. J. (1983) Rapid accumulation of inositol trisphosphate reveals that agonists hydrolyze polyphosphoinositides instead of phosphatidylinositol. Biochem. J. 212, 849–858.

25 Li, J., Edwards, P. C., Burghammer, M., Villa, C. and Schertler, G. F. X. (2004) Structure of bovine rhodopsin in a trigonal crystal form. J. Mol. Biol. 343, 1409–1438.

26 Salom, D., Lodowski, D. T., Stenkamp, R. E., Le Trong, I., Golczak, M., Jastrzebska, B., Harris, T., Ballesteros, J. A. and Palczewski, K. (2006) Crystal structure of a photoactivated deprotonated intermediate of rhodopsin. Proc. Natl. Acad. Sci. USA 103, 16123–16128.

27 Standfuss, J., Xie, G. F., Edwards, P. C., Burghammer, M., Oprian, D. D. and Schertler, G. F. X. (2007) Crystal structure of a thermally stable rhodopsin mutant. J. Mol. Biol. 372, 1179–1188.

28 Cherezov, V., Rosenbaum, D. M., Hanson, M. A., Rasmussen, S. G. F., Thian, F. S., Kobilka, T. S., Choi, H. J., Kuhn, P., Weis, W. I., Kobilka, B. K. and Stevens, R. C. (2007) High-resolution crystal structure of an engineered human beta(2)-adrenergic G protein-coupled receptor. Science 318, 1258–1265.

29 Rasmussen, S. G. F., Choi, H. J., Rosenbaum, D. M., Kobilka, T. S., Thian, F. S., Edwards, P. C., Burghammer, M., Ratnala, V. R. P., Sanishvili, R., Fischetti, R. F., Schertler, G. F. X., Weis, W. I. and Kobilka, B. K. (2007) Crystal structure of the human beta(2) adrenergic G-protein-coupled receptor. Nature 450, 383–384.

30 Aarons, E. J., Beddows, S., Willingham, T., Wu, L. J. and Koup, R. A. (2001) Adaptation to blockade of human immunodeficiency virus type 1 entry imposed by the anti-CCR5 monoclonal antibody 2D7. Virology 287, 382–390.

31 Dragic, A., Maric, Z. and Vigier, J. P. (1998) The energy spectrum of the hydrogen atom with magnetic spin-orbit and spin-spin interactions. Phys. Lett. A 237, 349–353.

32 Lee, B., Sharron, M., Blanpain, C., Doranz, B. J., Vakili, J., Setoh, P., Berg, E., Liu, G., Guy, H. R., Durell, S. R., Parmentier, M., Chang, C. N., Price, K., Tsang, M. and Doms, R. W. (1999) Epitope mapping of CCR5 reveals multiple conformational states and distinct but overlapping structures involved in chemokine and coreceptor function. J. Biol. Chem. 274, 9617–9626.

33 Kleinau, G., Claus, M., Jaeschke, H., Mueller, S., Neumann, S., Paschke, R. and Krause, G. (2007) Contacts between extracellular loop two and transmembrane helix six determine basal activity of the thyroid-stimulating hormone receptor. J. Biol. Chem. 282, 518–525.

34 Case, D. A. (2002) Molecular dynamics and NMR spin relaxation in proteins. Acc. Chem. Res. 35, 325–331.

35 Laskowski, R. A., Moss, D. S. and Thornton, J. M. (1993) Main-chain bond lengths and bond angles in protein structures. J. Mol. Biol. 231, 1049–1067.

36 Kosugi, S., Mori, T. and Shenker, A. (1996) The role of Asp(578) in maintaining the inactive conformation of the human lutropin/choriogonadotropin receptor. J. Biol. Chem. 271, 31813–31817.

37 Altenbach, C., Yang, K., Farrens, D. L., Farahbakhsh, Z. T., Khorana, H. G. and Hubbell, W. L. (1996) Structural features and light-dependent changes in the cytoplasmic interhelical E-F loop region of rhodopsin: A site-directed spin-labeling study. Biochemistry 35, 12470–12478.

38 Elling, C. E., Frimurer, T. M., Gerlach, L. O., Jorgensen, R., Holst, B. and Schwartz, T. W. (2006) Metal ion site engineering indicates a global toggle switch model for seven-transmembrane receptor activation. J. Biol. Chem. 281, 17337–17346.

39 Farrens, D. L., Altenbach, C., Yang, K., Hubbell, W. L. and Khorana, H. G. (1996) Requirement of rigid-body motion of transmembrane helices for light activation of rhodopsin. Science 274, 768–770.

40 Gether, U., Lin, S. S. and Kobilka, B. K. (1995) Fluorescent labeling of purified beta(2) adrenergic-receptor – Evidence for ligand-specific conformational changes. J. Biol. Chem. 270, 28268–28275.

41 Gether, U., Lin, S., Ghanouni, P., Ballesteros, J. A., Weinstein, H. and Kobilka, B. K. (1997) Agonists induce conformational changes in transmembrane domains III and VI of the beta(2) adrenoceptor. EMBO J. 16, 6737–6747.

42 Jensen, A. D., Guarnieri, F., Rasmussen, S. G. F., Asmar, F., Ballesteros, J. A. and Gether, U. (2001) Agonist-induced conformational changes at the cytoplasmic side of transmembrane segment 6 in the beta(2) adrenergic receptor mapped by site-selective fluorescent labeling. J. Biol. Chem. 276, 9279–9290.

43 Han, M., Lin, S. W., Minkova, M., Smith, S. O. and Sakmar, T. P. (1996) Functional interaction of transmembrane helices 3 and 6 in rhodopsin – Replacement of phenylalanine 261 by alanine causes reversion of phenotype of a glycine 121 replacement mutant. J. Biol. Chem. 271, 32337–32342.

44 Ho, H. H., Ganeshalingam, N., Rosenhouse-Dantsker, A., Osman, R. and Gershengorn, M. C. (2001) Charged residues at the intracellular boundary of transmembrane helices 2 and 3 independently affect constitutive activity of Kaposi's sarcoma-associated herpesvirus G protein-coupled receptor. J. Biol. Chem. 276, 1376–1382.

45 Hwa, J., Gaivin, R., Porter, J. E. and Perez, D. M. (1997) Synergism of constitutive activity in alpha(1)-adrenergic receptor activation. Biochemistry 36, 633–639.

46 Dunham, T. D. and Farrens, D. L. (1999) Conformational changes in rhodopsin – Movement of helix F detected by site-specific chemical labeling and fluorescence spectroscopy. J. Biol. Chem. 274, 1683–1690.

47 Lin, Z. L., Shenker, A. and Pearlstein, R. (1997) A model of the lutropin/choriogonadotropin receptor: Insights into the structural and functional effects of constitutively activating mutations. Protein Eng. 10, 501–510.

48 Ringkananont, U., Van Durme, J., Montanelli, L., Ugrasbul, F., Yu, Y. M., Weiss, R. E., Refetoff, S. and Grasberger, H. (2006) Repulsive separation of the cytoplasmic ends of transmembrane helices 3 and 6 is linked to receptor activation in a novel thyrotropin receptor mutant (M626I). Mol. Endocrinol. 20, 893–903.

49 Urizar, E., Claeysen, S., Deupi, X., Govaerts, C., Costagliola, S., Vassart, G. and Pardo, L. (2005) An activation switch in the rhodopsin family of G protein-coupled receptors – The thyrotropin receptor. J. Biol. Chem. 280, 17135–17141.

50 Altenbach, C., Klein-Seetharaman, J., Hwa, J., Khorana, H. G. and Hubbell, W. L. (1999) Structural features and light-

dependent changes in the sequence 59–75 connecting helices I and II in rhodopsin: A site-directed spin-labeling study. Biochemistry 38, 7945–7949.
51 Altenbach, C., Cai, K. W., Klein-Seetharaman, J., Khorana, F. G. and Hubbell, W. L. (2001) Structure and function in rhodopsin: Mapping light-dependent changes in distance between residue 65 in helix TM1 and residues in the sequence 306–319 at the cytoplasmic end of helix TM7 and in helix H8. Biochemistry 40, 15483–15492.
52 Altenbach, C., Klein-Seetharaman, J., Cai, K. W., Khorana, H. G. and Hubbell, W. L. (2001) Structure and function in rhodopsin: Mapping light-dependent changes in distance between residue 316 in helix 8 and residues in the sequence 60–75, covering the cytoplasmic end of helices TM1 and TM2 and their connection loop CL1. Biochemistry 40, 15493–15500.
53 Miura, S. and Karnik, S. S. (2002) Constitutive activation of angiotensin II type 1 receptor alters the orientation of transmembrane helix-2. J. Biol. Chem. 277, 24299–24305.
54 Sealfon, S. C., Chi, L., Ebersole, B. J., Rodic, V., Zhang, D., Ballesteros, J. A. and Weinstein, H. (1995) Related contribution of specific helix-2 and helix-7 residues to conformational activation of the serotonin 5-Ht2A receptor. J. Biol. Chem. 270, 16683–16688.
55 Zhou, W., Flanagan, C., Ballesteros, J. A., Konvicka, K., Davidson, J. S., Weinstein, H., Millar, R. P. and Sealfon, S. C. (1994) A reciprocal mutation supports helix-2 and helix-7 proximity in the gonadotropin-releasing-hormone receptor. Mol. Pharmacol. 45, 165–170.
56 Schulz, A. and Schoneberg, T. (2003) The structural evolution of a P2Y-like G-protein-coupled receptor. J. Biol. Chem. 278, 35531–35541.
57 Grasberger, H., Van Sande, J., Mahameed, A. H. D., Tenenbaum-Rakover, Y. and Refetoff, S. (2007) A familial thyrotropin (TSH) receptor mutation provides *in vivo* evidence that the inositol phosphates/Ca^{2+} cascade mediates TSH action on thyroid hormone synthesis. J. Clin. Endocrinol. Metab. 92, 2816–2820.
58 Xu, W., Sanz, A., Pardo, L. and Liu-Chen, L. Y. (2008) Activation of the mu opioid receptor involves conformational rearrangements of multiple transmembrane domains. Biochemistry 47, 10576–10586.
59 Cetani, F., Tonacchera, M. and Vassart, G. (1996) Differential effects of NaCl concentration on the constitutive activity of the thyrotropin and the luteinizing hormone chorionic gonadotropin receptors. FEBS Lett. 378, 27–31.